A LETTERS JOURNAL EXPLORING THE FRONTIERS OF PHYSICS

OFFPRINT

Effects of high-order fields of a tightly focused laser pulse on relativistic nonlinear Thomson scattered radiation by a relativistic electron

K. Lee, S. Y. Chung, S. H. Park, Y. U. Jeong and D. Kim

EPL, **89** (2010) 64006

A Letters Journal Exploring the Frontiers of Physics

March 2010

EPL, **89** (2010) 64006
doi: 10.1209/0295-5075/89/64006

www.epljournal.org

Effects of high-order fields of a tightly focused laser pulse on relativistic nonlinear Thomson scattered radiation by a relativistic electron

K. Lee[1(a)], S. Y. Chung[2(b)], S. H. Park[1], Y. U. Jeong[1] and D. Kim[2]

[1] *Quantum Optics Division, Korea Atomic Energy Research Institute - 1045 Daedeok Street, Yuseong, Daejeon 305-353, Korea*
[2] *Physics Department, Pohang University of Science and Technology - Pohang, Kyungbuk 790-784, Korea*

received 4 July 2009; accepted in final form 8 March 2010
published online 19 April 2010

PACS 41.60.-m – Radiation by moving charges
PACS 42.25.-p – Wave optics
PACS 42.65.-k – Nonlinear optics

Abstract – The effects of high-order fields of a tightly focused laser beam on the generation of relativistic nonlinear Thomson scattered radiations by a relativistic electron were investigated through numerical simulations. The high-order terms of the laser fields obtained by a series expansion in a diffraction angle were found to strongly affect the nonlinear Thomson scattered radiations by an increase in the transverse acceleration when electrons co-propagate with the laser pulse: the spectral range was broadened by a large factor and the angular power was enhanced by seven orders of magnitude compared to the corresponding values for a paraxial Gaussian laser beam. For electron energies higher than 200 MeV, the scaling exponent of the peak angular power with respect to the initial electron energy was also found to increase by a factor of 2.5 compared to the case of the paraxial laser beam.

Introduction. – The scattered radiations of a low-intensity laser pulse that are produced by a relativistic electron beam [1] have received considerable attention due to its monochromatic and intense characteristics, which can be useful in medical applications [2] and nuclear physics [3]. When the laser intensity becomes relativistic or the normalized vector potential, $a = eE_L/m_e\omega_o c$, exceeds unity, the motion of the electron becomes relativistically nonlinear; here, E_L is the laser field strength, ω_o the angular frequency of the laser field, e the electron charge, m_e the electron mass, and c the speed of light. This results in a radiation with a wide spectrum, known as relativistic nonlinear Thomson scattered (RNTS) radiation.

RNTS radiations have been investigated by both analytical and numerical ways [4–11], and the nonlinear harmonic spectra were obtained by irradiating atomic gases [12–15] and relativistic electron beams [16] with an intense laser pulse. Recently, Lee *et al.* proposed schemes for the generation of coherent RNTS radiations to produce an ultra-short X-ray pulse by utilizing ultra-thin solid targets [17] and relativistic electron beams co-propagating with a laser pulse [18]. A Compton back-scattering scheme has been recently devised for attosecond hard X-ray and γ-ray pulse [19].

All the analyses cited above are based on the plane-wave approximation. However, in actual experiments, the laser pulse should be focused to a spot that is 10 μm or less in diameter to produce the relativistic field strength. The focused laser pulse is usually modeled by a paraxial Gaussian beam or the zeroth-order solution of the wave equation [20]. Recently, it has been shown that the high-order terms of the laser field are critical to accurately calculate the dynamics of an electron [21] and ions [22] irradiated by the laser pulse when the beam waist is comparable to the laser wavelength. The high-order terms have also been considered in the laser-collider by counter-interacting an ultra-intense laser pulse with a gas of Ps atoms [23]. The spatial distribution of the high-order fields was found to strongly affect the RNTS radiations for an 80 MeV electron [24].

In this paper, on the basis of numerical-simulation results, we will describe how the generation of RNTS

(a) E-mail: klee@kaeri.re.kr
(b) Present address: Department of Electrical Engineering, Pusan National University - Pusan, 609-735, Korea.

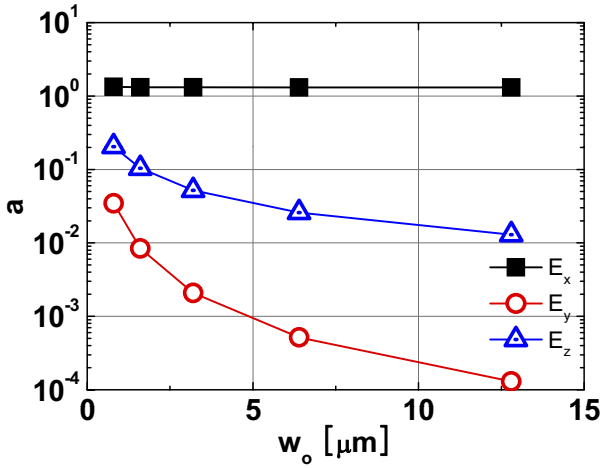

Fig. 1: (Colour on-line) Each component of the laser electric fields is plotted with respect to the beam waist size in units of the normalized vector potential. The laser field is evaluated at $(w_o/2,\ w_o/2,\ 0)$ for a zeroth-order laser intensity $a_0 = 2.2$.

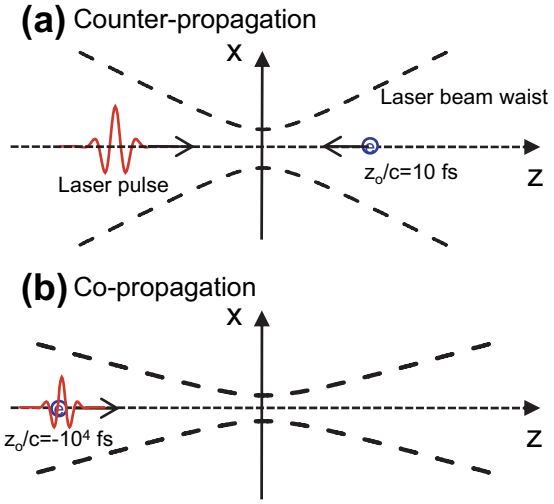

Fig. 2: (Colour on-line) Schematic diagrams for (a) the counter-propagation and (b) the co-propagation interaction scheme between a relativistic electron and a laser pulse.

radiations by a relativistic electron with an energy of 200–1000 MeV is affected by the high-order laser fields. In the case of a counter-propagation or a back-scattering scheme, such high-order terms are only small corrections to the paraxial laser beam. However, when an electron co-propagates with the laser pulse, the high-order terms of the laser field significantly enhances the RNTS radiations, and their effects get more significant as the beam waist size decreases. Different from the electron energy, which has been found to be significantly affected by odd-order fields or longitudinal laser fields [21], the RNTS radiation was found to be strongly enhanced by even-order fields, which increase the electron acceleration transverse to the laser propagation direction. Such high-order laser fields not only enhance the RNTS radiation power by a few orders of magnitude but also increase the scaling exponent of the RNTS radiation on the initial electron energy by a factor of 2.5 compared to that in the case of a paraxial laser beam.

Laser field beyond paraxial approximation. – The paraxial Gaussian laser beam is widely used for studying the interaction between an intense laser pulse and matter. However, it cannot be used any longer as the beam waist at the focal plane, w_o, becomes comparable to the laser wavelength, λ. Instead, series solutions of the wave equation expanded in terms of a diffraction angle, $\epsilon = w_o/Z_r$ ($Z_r = kw_o^2/2$: Rayleigh length, k: laser wave number) can be used once $\epsilon < 1$ is satisfied. Details on the derivation and the high-order laser fields can be found in refs. [25,26]. Figure 1 shows the peak amplitudes of three electric-field components, which were obtained by including the high-order laser fields up to the 7th order for a linearly polarized laser (in the x-direction) propagating in the $+z$-direction. It is seen that E_y and E_z get stronger as w_o decreases. The peak field strengths of E_y and E_z are 2.6% and 15% of E_x at $w_o = 1$ μm, respectively. In this calculation, $\lambda = 0.8$ μm and the zeroth-order field strength, $a_0 = 2.2$, were used for the laser pulse. The field strength was evaluated at $(w_o/2, w_o/2, 0)$. The results presented below were calculated in the $(z,\ x)$-plane, in which $E_y = B_z = 0$ [26].

Comparison of electron dynamics between the counter- and the co-propagation scheme. – The effect of the high-order laser fields on the electron dynamics was investigated for two different schemes, as shown in fig. 2. In the counter-propagation scheme, an electron with an initial energy of $E_o = 200$ MeV propagates in the $-z$-direction starting at $z_o/c = 10$ fs, while the laser pulse propagates in the $+z$-direction starting at $z_o/c = -10$ fs and is focused at $z = 0$. In the co-propagation scheme, the laser pulse and an electron begin to propagate together at $z_o/c = -10000$ fs toward the focal position. For the laser pulse, an ultra-short laser pulse with $\lambda = 0.8\,\mu$m, $a_0 = 10$, $\Delta t_{FWHM} = 5$ fs, and $w_o = 4\,\mu$m (in a hyperbolic secant temporal shape) was used. The dynamics of a relativistic electron were obtained by numerically solving the relativistic Newtonian equation of motion, and the formula for the generation of radiation by a moving charge was used for evaluating the RNTS radiations. The radiation reaction was neglected, which has been found to be significant if $4\gamma_0^2 \simeq a_0^2$ in the case of the counter-propagation scheme, where γ_0 is the initial relativistic gamma factor [27]. A detailed description can be found in ref. [28].

Figures 3 and 4 show how the dynamics of the electron are affected by the high-order laser fields in the counter-propagation and the co-propagation schemes, respectively. The numbers in the figures indicate the order up to which the high-order fields are included. In the counter-propagation scheme (fig. 3), the effect of the high-order laser fields on the dynamics is found to be negligible. In the figure, the result obtained for the zeroth-order field is

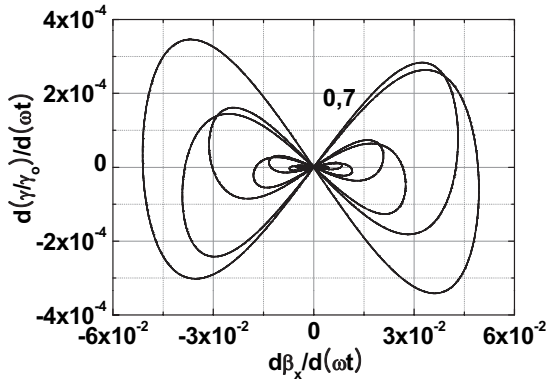

Fig. 3: For the counter-propagation case, the time derivatives of β_x and γ/γ_0 for the paraxial laser field and the laser field up to the 7th high order are compared. In this calculation, the laser pulse with $\lambda = 0.8\,\mu$m, $w_o = 4\,\mu$m, $a_0 = 10$, and $\Delta t_{FWHM} = 5$ fs interacts with an electron of $E_o = 200$ MeV. In the figure, the result obtained for only the zeroth-order field is superimposed on that for fields up to the 7th order being included; no difference is observed.

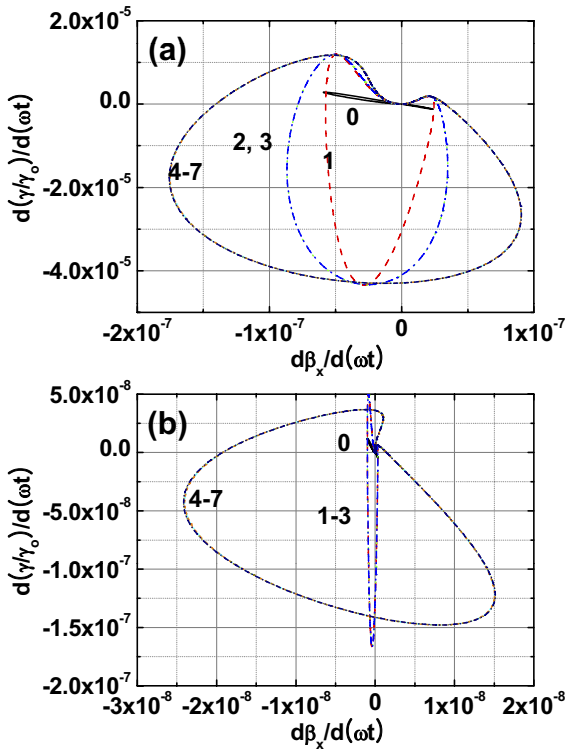

Fig. 4: (Colour on-line) For the co-propagating case, the time derivatives of β_x and γ/γ_0 are plotted by including the high-order laser fields for (a) 200 MeV and (b) 800 MeV electrons. The laser parameters used are the same as in fig. 3. The numbers on the plots indicate the order up to which the high-order fields are included.

superimposed on that for fields up to the 7th order being included; no difference is observed.

However, in the co-propagation scheme (fig. 4), the high-order fields significantly affect the dynamics by increasing the time derivative of energy and transverse acceleration. The inclusion of the first-order field enhances the variation of the electron energy or the relativistic gamma factor, γ, and the energy decreases below the initial values, which cannot happen in the case of the paraxial Gaussian beam. However, the effect of terms of order higher than one on the electron energy is negligible. The transverse acceleration is affected by even-order fields. In the case of 200 MeV electron (fig. 4(a)), the 2nd-order and 4th-order fields affect the transverse acceleration, while only the 4th-order laser field affects the transverse acceleration in the case of 800 MeV electron (fig. 4(b)). The fields of order higher than four are considered to be small corrections.

These variations in the electron dynamics caused by the high-order fields can be understood by examining the equation of motion for the co-propagation ($\beta_z \simeq +1$) and the counter-propagation ($\beta_z \simeq -1$) schemes. In the $(z,\ x)$-plane, only E_x, E_z, and B_y are considered since $E_y = B_z = 0$ at $y = 0$; then, γ can be obtained by neglecting terms higher than the first order:

$$\frac{\gamma}{\gamma_0} \simeq \begin{cases} \dfrac{1+\alpha_0^2}{1-2\gamma_0\Delta\alpha_1}, & \text{for } \beta_z \simeq +1, \\ 1+\eta_0^2 - \dfrac{\Delta\alpha_1}{2\gamma_0}\left[1-\eta_0^2\right], & \text{for } \beta_z \simeq -1, \end{cases} \tag{1}$$

where α_0 and $\Delta\alpha_1$ are the integrals of the zeroth- and the first-order laser field in the unit of normalized vector potential over the phase ($\phi = \omega_o t - k_o z(t)$), respectively, and $\eta_0^2 = (1+\alpha_0^2)/2\gamma_0^2$. In the derivation of the above equations, $|\beta_x| \ll 1$, $|\beta_z| \simeq 1$, and $\gamma \gg 1$. This shows that in the co-propagation scheme ($\beta_z \simeq +1$), γ can be larger or smaller than its initial values, depending on the sign of $\Delta\alpha_1$, but γ varies only above its initial value, if $\Delta\alpha_1 = 0$. However, in the counter-propagation scheme, since $\Delta\alpha_1/2\gamma_0 \ll 1$, the high-order fields are only considered as a small correction.

The equation of motion for the transverse velocity can be approximated as follows:

$$\frac{\mathrm{d}\,(\gamma\beta_x)}{\mathrm{d}\tau} \simeq \begin{cases} \dfrac{a_0}{2\gamma^2} + (\Delta a_e - \Delta b_e), & \text{for } \beta_z \simeq +1, \\ 2a_0 + (\Delta a_e + \Delta b_e), & \text{for } \beta_z \simeq -1, \end{cases} \tag{2}$$

where Δa_e and Δb_e are the even-order terms of the electric and magnetic fields, respectively, and $\tau = \omega t$. The transverse fields contain only even-order fields while the longitudinal fields contain odd-order fields [26]. From eq. (2), the effect of the high-order fields for different propagation schemes is more clearly observed. In the case of the counter-propagation scheme ($\beta_z \simeq -1$), the high-order fields are only a small correction to the zeroth-order field. However, in the case of the co-propagation scheme ($\beta_z \simeq +1$), because of the factor of $1/2\gamma^2$ in front of a_0, the contribution of the high-order fields could be comparable to that of the zeroth-order fields; this significantly alters the electron dynamics. It is the difference between the high-order transverse electric and magnetic fields that causes such a dramatic change. These observations show

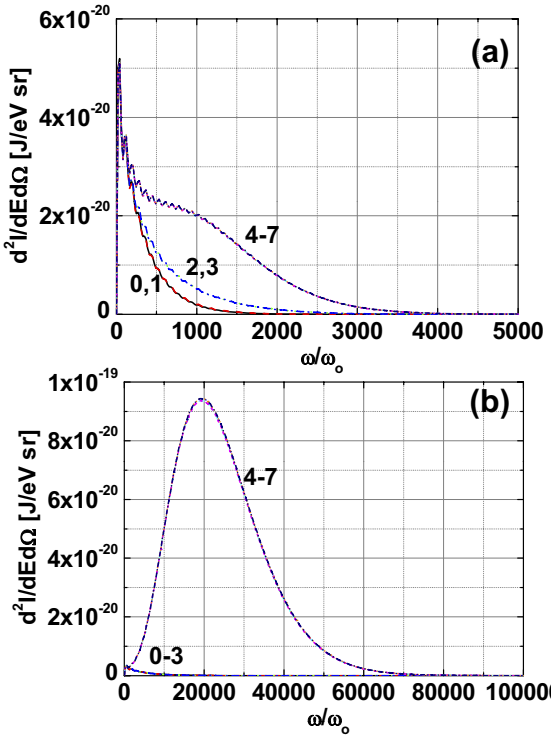

Fig. 5: (Colour on-line) For the dynamics shown in fig. 4, the angular radiation spectra for (a) 200 MeV and (b) 800 MeV are calculated and plotted, including the high-order fields. The spectra were obtained in the direction of maximum radiation, which is the same as that of the laser propagation.

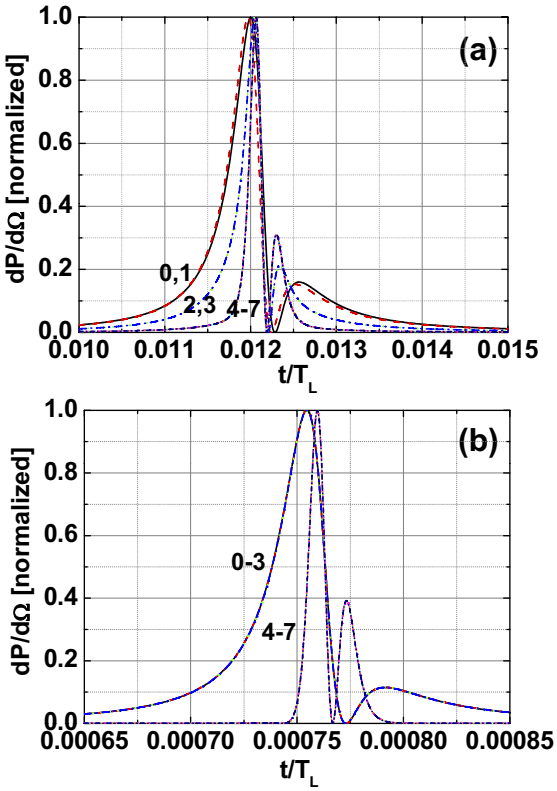

Fig. 6: (Colour on-line) For the case shown in fig. 5, the angular powers are plotted for (a) 200 MeV and (b) 800 MeV electrons. Each plot is normalized to its peak value for comparison. The peak values in ascending order are 11.0, 11.4, 22.6, 22.6, 94.1, 94.1, 94.7, and 94.7 W/sr for the 200 MeV case and 192, 192, 193, 193, 1.14×10^5, 1.14×10^5, 1.15×10^5, and 1.15×10^5 W/sr for the 800 MeV case. T_L is the period of the laser oscillation (2.7 fs).

that in the co-propagation scheme, the inclusion of the high-order terms of the laser field considerably alters the dynamics in such a manner that the magnitudes of the electron's acceleration are enhanced, which is essential to the strong RNTS radiations.

The difference between the cases of 200 MeV and 800 MeV electrons in the co-propagation scheme is caused by the spatial distribution of the 2nd- and the 4th-order laser fields. As the electron energy increases, the deflection of the electron from the axis decreases. Thus, the contribution of the 4th-order field, which contains a constant term, dominates that of the 2nd-order field, which vanishes on the propagation axis.

RNTS radiations in the co-propagation scheme. – Calculated from the dynamics shown in fig. 4, the angular spectral intensity and the temporal profile of the angular power in the direction of maximum radiation are plotted in figs. 5 and 6, respectively. Note that the spectral intensity of the RNTS radiation increases by more than a factor of 10 and the spectral range becomes about 7 times wider in the case of 800 MeV (fig. 5 (b)). Since the electron experiences only a single sweep of the laser pulse near the focal region, the spectrum appears as a continuum instead of modulated harmonic spectra [28]. The increase in the spectral bandwidth results in a decrease in the pulse width of the RNTS radiation, as shown in fig. 6. The peak angular power is also enhanced by more than two orders of magnitude. The results also show that it is the even-order laser fields that significantly enhance the RNTS radiations through the increase in the transverse acceleration (fig. 4). These observations have been further developed to a physical scheme for the generation of attosecond X-ray pulse [29].

For the co-propagation scheme, the enhancement in the RNTS radiations by the inclusion of high-order fields for different beam waist sizes is shown in fig. 7. The contribution from the 4th-order field becomes more significant as the beam waist size decreases, increasing the peak angular power by a factor of 10^7 at $w_o = 1$ μm for 800 MeV. In the case of 200 MeV, the contribution of the first- and the second-order fields to the radiation can be considered to be constant for $w_o < 10\,\mu$m. As expected, the effect of the high-order terms becomes negligible for large beam waist sizes of $w_o > 10\,\mu$m.

The change in the effect of the high-order laser fields on the RNTS radiations with the initial electron energy was investigated for the co-propagation scheme. The result is shown in fig. 8, for a beam waist size of $w_o = 5\,\mu$m. Figure 8(a) shows that the inclusion of high-order fields

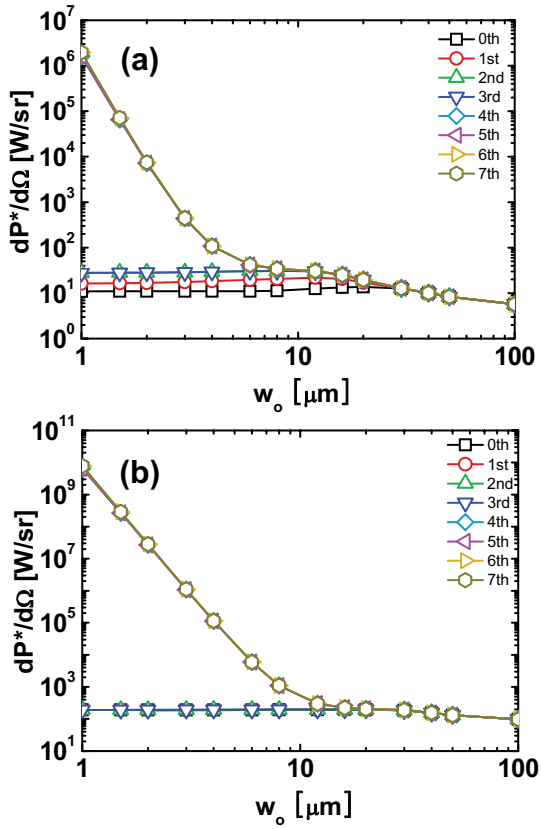

Fig. 7: (Colour on-line) For the co-propagation scheme, the change in the peak angular power with respect to the beam waist size is plotted for (a) 200 MeV and (b) 800 MeV electrons while including the high-order laser fields.

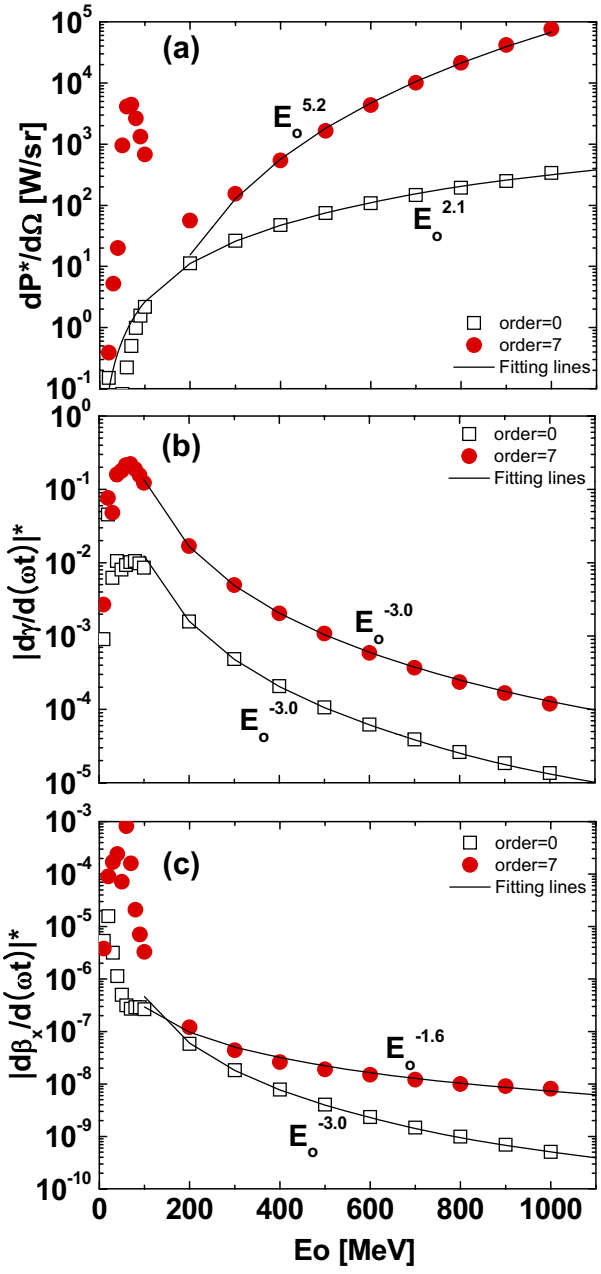

Fig. 8: (Colour on-line) For the co-propagation scheme, the peak values of (a) the angular power in the direction of maximum radiation, (b) $|\mathrm{d}\gamma/\mathrm{d}\tau|$, and (c) $|\mathrm{d}\beta_x/\mathrm{d}\tau|$ *vs.* the initial electron energy for the paraxial laser beam and the laser beam including fields up to the 7th-order field are compared. For initial energies as high as 200 MeV and above, the scaling laws are obtained by a numerical fitting.

of a laser pulse not only enhances the radiation power but also increases the scaling exponent by a factor of approximately 2.5 for $E_o > 200\,\mathrm{MeV}$. For $E_o < 200\,\mathrm{MeV}$, the peak angular power shows interesting behavior with respect to E_o; this behavior has been found to be caused by the nice match between the spatial distribution of the high-order laser fields and the electron's trajectory near focal point for a low-energy electron [24].

To understand the enhancement of the scaling, the peak values of $|\mathrm{d}\gamma/\mathrm{d}\tau|$ and $|\mathrm{d}\beta_x/\mathrm{d}\tau|$ are also investigated as shown in figs. 8(b) and (c), respectively. In the case of $|\mathrm{d}\gamma/\mathrm{d}\tau|$, even though the value increases by an order of magnitude, the scaling of E_o^{-3} does not change with the inclusion of high-order fields. In contrast, in the case of $|\mathrm{d}\beta_x/\mathrm{d}\tau|$, the scaling exponent changes from E_o^{-3} to $E_o^{-1.6}$.

The scaling laws can be understood from eq. (2) for $\beta_z \simeq +1$. For high-energy electrons with $E_o > 200\,\mathrm{MeV}$, γ can be approximated as a constant, namely, $\mathrm{d}(\gamma\beta_x)/\mathrm{d}\tau \simeq \gamma\mathrm{d}\beta_x/\mathrm{d}\tau$, since the change in γ is very small. Then, eq. (2) can be written as

$$\frac{\mathrm{d}\beta_x}{\mathrm{d}\tau} \sim \frac{1}{\gamma^3}\left[\frac{a_0}{2} + \gamma^2\left(\Delta a_e - \Delta b_e\right)\right]. \tag{3}$$

This leads to the scaling of $|\mathrm{d}\beta_x/\mathrm{d}\tau| \propto \gamma^{-3}$ when only the a_0 term is considered, but one can expect that the scaling exponent is in the range from -3 to -1 when the high-order fields are included. The scaling of the angular power with respect to E_o can also be analyzed by considering the total radiation power from an electron [30],

$$P(t') = \frac{2}{3}\frac{e^2}{c}\omega^2\gamma^6\left[\left(\dot{\vec{\beta}}\right)^2 - \left(\vec{\beta}\times\dot{\vec{\beta}}\right)^2\right], \tag{4}$$

where t' is the retarded time and is associated with the time measured at a detector, t, as $\mathrm{d}t = \mathrm{d}t'(1 - \hat{n}\cdot\beta(\vec{t'}))$,

where $\hat{n}$ is the direction in which the radiation is measured. Since the strongest radiation appears near the z-axis, it can be approximated as $\mathrm{d}t' \simeq 2\gamma^2 \mathrm{d}t$. Considering the angular divergence of $\Delta\Omega \sim \gamma^{-2}$, the angular power at the detector can be approximated as

$$\frac{\mathrm{d}P}{\mathrm{d}\Omega} \propto \gamma^8 \left(\frac{\mathrm{d}\beta_x}{\mathrm{d}\tau}\right)^2. \tag{5}$$

In this derivation, $\gamma^4(\mathrm{d}\beta_x/\mathrm{d}\tau)^2 \gg (\mathrm{d}\gamma/\mathrm{d}\tau)^2$ is used. By applying the scaling law of $|\mathrm{d}\beta_x/\mathrm{d}\tau|$ obtained in the simulation, this equation yields the scaling of the angular power with respect to the initial energy as E_o^2 and $E_o^{4.8}$ for laser fields including only the zeroth-order term and the high-order terms, respectively. The exponents are comparable to the numerically obtained values of 2.1 and 5.2, respectively.

Since the spatial distribution of the high-order fields, peaked near $x_o \simeq w_o$, are different from the zeroth-order one [26], one could expect stronger RNTS radiations might appear for off-axis electron. This effect will be thoroughly investigated in a separate paper for a real application.

Summary. – The generation of RNTS radiations of a focused, intense laser pulse by a relativistic electron was investigated by performing numerical simulations using the series solution of the wave equation for the laser pulse. In the counter-propagation scheme, the high-order laser fields contribute only small correction. However, in the co-propagation scheme, the enhancement of the time derivatives of γ and β_x by the high-order terms of the laser field was found to significantly enhance the peak angular power in the RNTS radiations by orders of magnitude for a beam waist size of $w_o < 10\,\mu$m. The high-order terms of the laser field not only enhance the RNTS radiation power but also increase the scaling exponent with respect to the electron energy by a factor of 2.5 due to the increase in the transverse acceleration.

* * *

This work has been supported through the Basic Research Promotion Grant funded by the Korean Research Foundation (Grant No. KRF-2008-313-C00356) and through the Global Research Laboratory Program (Grant No. 2009-00439) funded by the National Research Foundation of Korea (NRF).

REFERENCES

[1] Brown W. J., Anderson S. G., Barty C. P. J., Betts S. M., Booth R., Crane J. K., Cross R. R., Fittinghoff D. N., Gibson D. J., Hartemann F. V., Hartouni E. P., Kuba J., Le Sage G. P., Slaughter D. R., Tremaine A. M., Wootton A. J., Springer P. T. and Rosenzweig J. B., *Phys. Rev. ST Accel. Beams*, **7** (2004) 060702.

[2] Girolami B., Larsson B., Preger M., Schaerf C. and Stepanek J., *Phys. Med. Biol.*, **41** (1996) 1581.

[3] Weller H. R. and Ahmed M. W., *Mod. Phys. Lett. A*, **18** (2003) 1569.

[4] Esarey E., Ride S. K. and Sprangle P., *Phys. Rev. E*, **48** (1993) 3003.

[5] Hartemann F. V. and Kerman A. K., *Phys. Rev. Lett.*, **76** (1996) 624.

[6] Salamin Y. I. and Faisal F. H., *J. Phys. A*, **31** (1998) 1319.

[7] Ueshima Y., Kishimoto Y., Sasake A. and Tajima T., *Laser Part. Beams*, **17** (1999) 45.

[8] Lee K., Cha Y. H., Shin M. S., Kim B. H. and Kim D., *Opt. Express*, **11** (2003) 309.

[9] Hartemann F. V., Gibson D. J. and Kerman A. K., *Phys. Rev. E*, **72** (2005) 026502.

[10] Koga J., Esirkepov T. Zh. and Bulanov S. V., *Phys. Plasmas*, **12** (2005) 093106.

[11] Avetissian H. K. and Mkrtchian G. F., *Phys. Rev. E*, **65** (2002) 046505.

[12] Chen S-Y., Maksimchuk A. and Umstadter D., *Nature (London)*, **396** (1998) 653.

[13] Chen S-Y., Maksimchuk A., Esarey E. and Umstadter D., *Phys. Rev. Lett.*, **84** (2000) 5528.

[14] Banerjee S., Valenzuela A. R., Shah R. C., Maksimchuk A. and Umstadter D., *Phys. Plasmas*, **9** (2002) 2393.

[15] Ta Phuoc K., Rousse A., Pittman M., Rousseau J. P., Malka V., Fritzler S., Umstadter D. and Hulin D., *Phys. Rev. Lett.*, **91** (2003) 195001.

[16] Bula C., McDonald K. T., Prebys E. J., Bamber C., Boege S., Kotseroglou T., Melissinos A. C., Meyerhofer D. D., Ragg W., Burke D. L., Field R. C., Horton-Smith G., Odian A. C., Spencer J. E., Walz D., Berridge S. C., Bugg W. M., Shmakov K. and Weidemann A. W., *Phys. Rev. Lett.*, **76** (1996) 3116.

[17] Lee K., Kim B. H. and Kim D., *Phys. Plasmas*, **12** (2005) 043107.

[18] Lee K., Park S. H. and Jeong Y. U., *J. Korean Phys. Soc.*, **48** (2006) 546.

[19] Chung S., Yoon M. and Kim D., *Opt. Express*, **17** (2009) 7853.

[20] Diels J.-C. and Rudolph W., *Ultrashort Laser Pulse Phenomena* (Academic Press, London).

[21] Salamin Y. I. and Keitel C. H., *Phys. Rev. Lett.*, **88** (2002) 095005.

[22] Salamin Y. I., Harman Z. and Keitel C. H., *Phys. Rev. Lett.*, **100** (2008) 155004.

[23] Liu C., Kohler M. C., Hatsagortsyan K. Z., Müller C. and Keitel C. H., *New J. Phys.*, **11** (2009) 105045.

[24] Lee H., Chung S., Lee K. and Kim D., *New J. Phys.*, **10** (2008) 093024.

[25] Davis L. W., *Phys. Rev. A*, **19** (1979) 1177.

[26] Salamin Y. I., *Appl. Phys. B*, **86** (2007) 319.

[27] Di Pizza A., Hatsagortsyan K. Z. and Keitel C. H., *Phys. Rev. Lett.*, **102** (2009) 254802.

[28] Lee K., Cha Y. H., Shin M. S., Kim B. H. and Kim D., *Phys. Rev. E*, **67** (2003) 026502.

[29] Kim D., Lee H., Chung S. and Lee K., *New J. Phys.*, **11** (2009) 063050.

[30] Jackson J. D., *Classical Electrodynamics,* 2nd edition (Wiley, New York) 1975.